frontiers | Frontiers in Physics

TYPE Review
PUBLISHED 05 February 2024
DOI 10.3389/fphy.2024.1304896

OPEN ACCESS

EDITED BY
Iain Sedgwick,
Rutherford Appleton Laboratory,
United Kingdom

REVIEWED BY
Marcus French,
Rutherford Appleton Laboratory,
United Kingdom
Arkadiusz Dawiec,
Soleil Synchrotron, France

*CORRESPONDENCE
Erik Fröjdh,
erik.frojdh@psi.ch

RECEIVED 30 September 2023
ACCEPTED 09 January 2024
PUBLISHED 05 February 2024

CITATION
Fröjdh E, Bergamaschi A and Schmitt B (2024), Single-photon counting detectors for diffraction-limited light sources.
Front. Phys. 12:1304896.
doi: 10.3389/fphy.2024.1304896

Single-photon counting detectors for diffraction-limited light sources

Erik Fröjdh*, Anna Bergamaschi and Bernd Schmitt

Paul Scherrer Institut, Villigen, Switzerland

When first introduced, single-photon counting detectors reshaped crystallography at synchrotrons. Their fast readout speed enabled, for example, shutter-less data collection and fine slicing of the rotation angle and boosted the development of new experimental techniques like ptychography. Under optimal conditions, single-photon counting detectors provide an unlimited dynamic range with image noise only limited by the Poisson statistics of the incoming photons. Counting the pulses from individual photons, essentially what made the detectors so successful, also causes the main drawback, which is the loss of efficiency at high photon fluxes due to pulse pileup in the analog front end. To fully take advantage of diffraction-limited light sources, the next-generation single-photon counters need to improve their count rate capabilities in the same order of magnitude as the increased flux. Moreover, fast frame rates (a few kHz) are required to cope with the shorter dwell time achievable, thanks to the higher flux. Detector architecture with multiple comparators and counters can open new possibilities for energy-resolved imaging, while interpixel communication can overcome the issues arising from charge sharing and reduce the loss of efficiency at the pixel corners. Coupling single-photon counting detectors to high-Z sensors for hard X-ray detection (>20 keV) and to low-gain avalanche diodes (LGADs) for soft X-rays is also necessary to make use of the increased coherence of the new light sources over the full radiation spectrum. In this paper, we present possible strategies to improve the performance of single-photon counting detectors at the fourth-generation synchrotron sources and compare them to charge integrating detectors.

KEYWORDS

hybrid detectors, x-ray detectors, pixel detectors, single-photon counting, synchrotron

1 Introduction

The idea of hybrid pixel detectors originated around the end of 1980s from within the particle physics community [1]. The first fully functional hybrid pixel detector was tested in the Omega-Ion experiment (WA94) in 1991 [2], and larger installations soon followed [3; 4]. Scientists realized early that hybrid detectors also would be a good fit for X-ray imaging [5; 6], and several groups [7; 8] including PSI Brönnimann et al. [9] started working on dedicated detectors. The development of single-photon counting (SPC) hybrid pixel detectors at PSI was motivated by the needs of diffraction applications at the Swiss Light Source, and most of the know how came from working on the original pixel chip for the CMS experiment at the LHC [10]. The PILATUS 1-M detector was the first large-

area SPC detector dedicated to macromolecular crystallography [11]. It comprised 18 multi-chip modules for a total of 288 readout chips covering 21 × 24 cm^2.

Since their introduction, single-photon counting detectors have transformed data collection at synchrotrons. Replacing slower and less-sensitive detectors, they enable, for example, fine slicing of the rotation angle and shutter-less data collection [12; 13; 14] and now underpin many modern measurement techniques like ptychography [15]. Currently, most scattering beamlines at synchrotrons rely on SPC detectors like PILATUS [16; 17], EIGER [18; 19], XPAD3S [20], UFXC32k [21; 22], MEDIPIX [23; 24; 25], and MYTHEN [26]. SPC detectors can also be used for electron detection, for example, in low-energy electron microscopy and photoemission electron microscopy [27].

A pixel in a typical single-photon counting detector consists of a charge-sensitive preamplifier, shaper, comparator, and counter. When the analog signal exceeds a certain threshold, it is counted as a photon. If the threshold is high enough compared to the electronic noise (at least five times the RMS) and the photon energy is similarly higher than the threshold, it is possible to detect photons with a high efficiency and extremely good noise rejection [28]. Given that when a photon is absorbed between two pixels, its charge is shared between them, the threshold should be set at half of the photon energy in order to maximize the number of detected X-rays while avoiding double counts [16]. The electronic noise defines the minimum detectable energy at about 10 times the RMS of the electronic noise [26].

Another important parameter is the threshold dispersion, i.e., the accuracy of tuning the threshold at the same energy level for all the channels. Threshold equalization methods must be implemented to compensate for mismatches between channels in the analog chain, affecting mainly the gain and the baseline level. Since the threshold is normally set as a voltage, the threshold equalization circuitry is then implemented by adding an additional *trim* threshold to the global threshold common to all channels of the chip (or of the detector module). The *trim* digital-to-analog converter (DAC) has a resolution ranging between 3 and 6 bits, and usually, the range of the voltage available for trimming can be tuned by using an external voltage, as in [29]. Recently, trimming architectures capable of tuning the gain and offset of the analog chain by acting at the shaper level have been demonstrated by [30]. Threshold equalization strategies can either be implemented by optimizing the count dispersion using a flat illumination, as in [31], or by equalizing the gain at a certain energy, as in [32]. The energy resolution of the detector, i.e., the accuracy to define the threshold to discriminate photons of different energies, is given by the quadratic sum of the electronic noise and of the threshold dispersion [33]. This can be exploited, for example, in the case of fluorescence radiation emitted by the sample, which can be rejected by setting the threshold between the main beam energy and the fluorescence line.

Since SPC detectors do not provide any information about the energy of the photons, their performance is not ideal in case of a polychromatic radiation spectrum. However, also in this case, by assigning the same weight to each detected photon, their performance outdoes charge-integrating detectors, where the weight of the photons is proportional to their energy, resulting in a reduction of the image contrast [34] or in stronger high harmonic contamination in the case of diffraction applications.

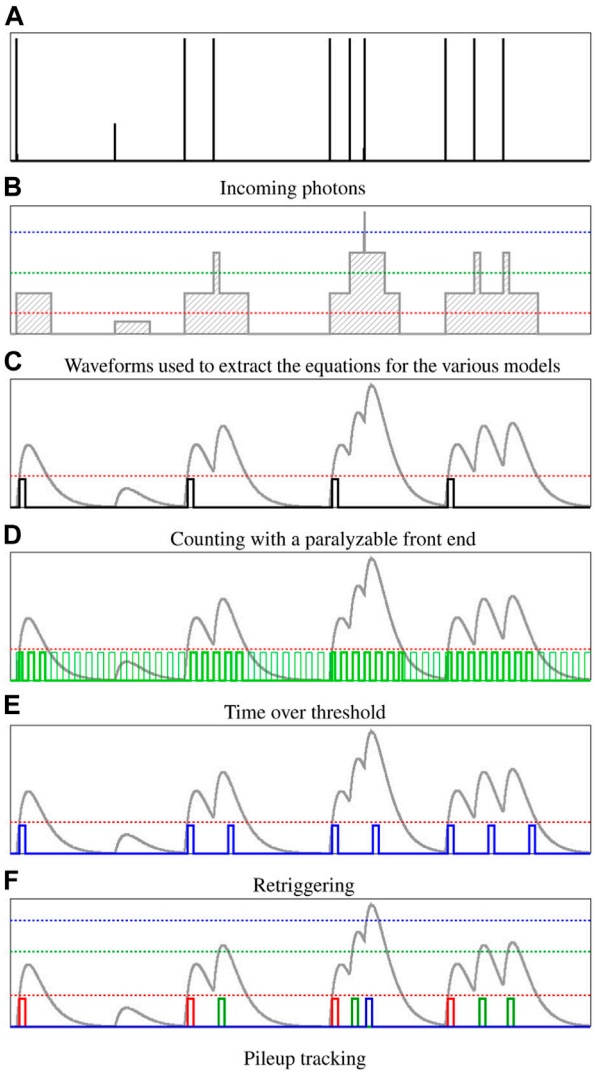

FIGURE 1
(A,B) Method to compare different strategies for mitigating the pulse pileup: **(C)** normal counting (reference), **(D)** time-over-threshold, **(E)** retriggering, and **(F)** pileup tracking. The *x*-axis refers to time, while the *y*-axis represents the height of the analog signal.

The readout of the detector is completely digital, and it does not add any noise to the data. Therefore, in ideal conditions, SPC detectors provide *noiseless* data, where the image quality is only limited by the Poisson fluctuations of the number of incident photons. SPC detectors can provide perfect linearity and virtually infinite dynamic range, only limited by the exposure time since it is possible to sum frames without adding noise. Lower bit depths or partial readout of the counters allow extremely high frame rates, for example, 20 kfps for EIGER [35] and 56 kfps for UFXC32k [21], while data compression can help achieve frame rates higher than 100 kHz [36]. A further improvement in speed can be achieved by defining a region of interest [37].

Using an electronic shutter, SPC detectors can be gated with a time resolution usually of a few tens of ns. This is of particular interest for pump–probe experiments since the signal from multiple probes can be accumulated at high frequencies without the need to

read out the detector in between the gates. With the hybrid fill pattern of synchrotrons, it is possible to gate the isolated bunch and obtain a time resolution limited by the duration of the bunch and by its jitter [21; 38].

Despite their success, single-photon counters still suffer from one major inherent weakness since the pulse processing front-end makes them susceptible to a loss of efficiency due to the pileup (Figure 1C). For this reason, SPC detectors require significant improvements in order to best use the increased brilliance of the fourth-generation synchrotron sources. In the following section, we will discuss the main ideas behind the development of the next-generation SPC detectors and look at their expected performance compared to charge-integrating detectors, initially developed for X-ray free-electron lasers (XFELs) but increasingly also used at synchrotrons. We will investigate the count rate capability (i.e., the linearity of the detector as a function of the number of photons per second), the spatial resolution, and strategies for extending the detectable energy range toward both lower- and higher-energy photons using advanced sensors.

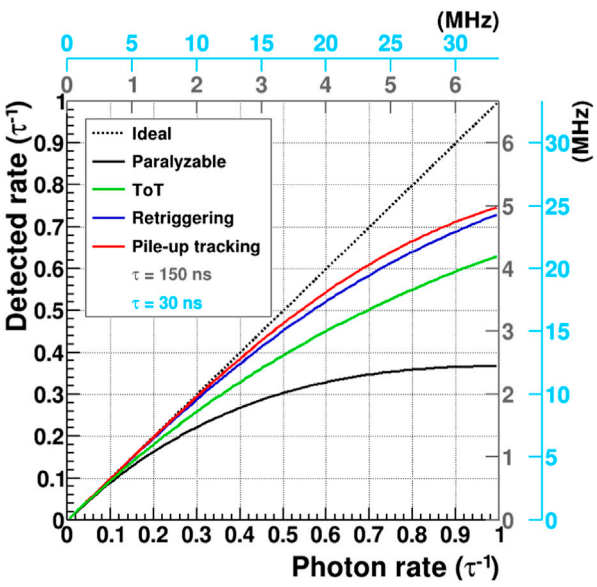

FIGURE 2
Detected rate as a function of the photon rate for a single-photon counting detector calculated using Eqs 1–4, covering the different solutions described in section 2.2. The rate is expressed as the reciprocal of the shaping time per pixel per second. The gray and the blue secondary axes compare the performance in Mphotons/pixel/s of SPC detectors with τ =150 ns and τ =30 ns, respectively.

2 Discussion

The readout electronics of hybrid pixel detectors benefits from the advances in CMOS technology. By exploiting more advanced, smaller technology nodes with a higher transistor density, it is possible to integrate more functionalities in the pixel and target smaller pixel pitches, still with an acceptable power consumption. Moreover, by implementing advanced logic on-chip, taking advantage of the synthesized digital circuitry, the fully digital data can be processed in hardware to reduce the data throughput or speed up the readout.

In this section, we discuss the major trends in SPC detector development toward diffraction-limited light sources, namely, the possibility of having multiple comparators and counters per pixel with independent thresholds and enabling signals; the development of methods to reduce the loss of efficiency at high count rates; the goal of achieving a high spatial resolution either using smaller pixels or exploiting advanced inter-communication between pixels; and the possibility to combine SPC detectors with novel sensor technologies in order to cover an energy range spanning from soft to hard X-rays. Finally, we compare SPC with charge-integrating detectors, highlighting the strengths and weaknesses of both readout modes, and discuss the challenge of handling the data produced by fast large-area detectors.

2.1 Multiple comparators and counters

Thanks to the miniaturization of electronic components using advanced CMOS technologies, several comparators, each with an individual threshold, trimbits, and counter with independent gates can be allocated in the same pixel. The comparators and counters can be connected using the logic of varying complexity, and even inter-pixel communication can be implemented. The independent thresholds give access to different energy bins, the independent gates to different time windows.

The main application exploiting the independent thresholds is energy binning [39]. It can be used at polychromatic X-ray sources and is exploited in clinical CT systems [40]. However, energy binning can also be used at synchrotron beamlines for high harmonic and fluorescence suppression or detection. As long as the spectroscopic capabilities do not degrade at high fluxes, the energy discrimination capabilities can be used to operate in the pink beam mode, i.e., using a larger bandwidth without monochromatizing optics, to isolate the full undulator harmonic. The energy resolution depends not only on the noise and on the threshold dispersion but also on charge sharing. Therefore, larger pixel sizes and charge-sharing suppression methods (see section 2.3) are an advantage for energy binning. The multiple thresholds can also be exploited to improve the count rate capability, as described in section 2.2.3. Complex digital circuitry and inter-pixel communication can be used, for example, for interpolation to achieve a sub-pixel resolution, as highlighted in section 2.3.

The independent gates enabling the counters can be used to perform measurements in different time windows. Given that the reaction being studied happens on the same time scale, or slower, than the shortest gate that can be applied (normally tens of nanoseconds), it is possible to probe at multiple times and thus reduce the duration of the experiment proportionally to the number of counters compared to a single probe. Moreover, it is possible to acquire pumped and unpumped data alternating in time and, therefore, correct for possible low-frequency drifts of the system [41]. Ideally, a single comparator is connected to the multiple independent counters to minimize mismatches between different probes since the changes in the sample can be subtle (~1% or less).

2.2 Count rate capability

Single-photon counting detectors present a paralyzable behavior due to the pileup of the signal of photons arriving close to each other in time. This means that after detecting a photon, the detector is insensitive for a defined time (dead time), and a photon detected during this interval will not be counted and will also restart the dead time. As a consequence, with the increasing rate, the detector will reach a saturation point where it will be incapable of recording any event at all. To fully capitalize on the increased brilliance of the fourth-generation light sources, count rate capabilities up to 100 Mphotons/pixel/second are required. In the following section, we discuss and compare the new approaches that have been proposed to extend the usability of SPC detectors at next-generation synchrotron sources. They rely on the idea that when two or more photons pile up, the analog signal has a larger amplitude and longer duration. The working principle of various methods is shown in Figure 1, while Figure 2 shows the comparison of their performance in terms of count rate capability. The secondary axes quantify the performance in terms of impinging photon rate for 150-ns and 30-ns shaping times.

Usually, the count rate capability of an SPC detector is modeled according to the parameter τ, which is proportional to the shaping time of the analog chain. It scales inversely with the shaping time of the analog signal, which is usually a compromise between the noise and gain of the detector. Therefore, the count rate performance tends to improve at high energies, where a lower gain can be used, and a loss of signal due to ballistic deficit can also be afforded. Another approach to obtain a fast shaping is active reset, as demonstrated by [42]. Faster shaping time and active reset cause a high power consumption, which is sometimes unacceptable for large readout chips with tens of thousands of pixels. Current single-photon counters exhibit a τ of 30–150 ns, which translates to approximately 2–10 Mcounts/pixel/s. The KITE ASIC from DECTRIS has been designed for electron microscopy with extremely short signal pulses of 6 ns FWHM [36]. This is possible thanks to the fast settings and low gain allowed by the extremely large signal generated by high-energy electrons, as well as the small size with no buttability, which allows high power consumption and optimal power distribution.

It is important to highlight that the count rate capability of SPC detectors depends on the photon distribution, i.e., on the filling pattern of the light source [43]. The actual time structure varies between synchrotrons and can, in many cases, be tuned, from a few isolated bunches to the quasi continuous mode, in order to optimize for certain experiments. Filling patterns with fewer bunches spaced more than the shaping time of the analog signal usually allow better performance, the rate correction present requires a simpler calibration of the parameters, and the methods explained in the following are more effective since they are less subjected to statistical fluctuations in the photon time distribution. However, in this case, the equations reported for the count rate corrections must be modified due to the different photon distribution.

For modeling the count-rate corrections presented in this section, a Poisson-like photon distribution is assumed, with no charge sharing and τ-wide rectangular pulse shape, where τ approximates the time-over-threshold of the analog pulse, as shown in Figure 1B. For a simple SPC detector, the paralyzable detector model applies for converting from the impinging photon rate ϕ to the measured flux φ [44]:

$$\varphi = \phi e^{-\phi\tau} \tag{1}$$

Despite being a simplified description of the pileup, this approach allows to model analytically the corrections needed to convert the detected signal into the impinging photon rate. The real corrections will depend also on other factors, such as the fill pattern of the photon source, charge sharing, and—in particular—on the shape of the analog signal, which should be optimized depending on the strategy chosen to improve the count rate capability.

2.2.1 Time-over-threshold

The time-over-threshold (ToT) readout measures the time duration of the analog signal above the threshold by providing a clock to each pixel and incrementing the counter while the signal is above the threshold (Figure 1D). This method is usually applied to measure the energy of the impinging particle, as in the TIMEPIX detectors [45]. However, to improve the energy resolution, slow shaping times are usually implemented, in contrast with the requirements to obtain a high count rate capability in SPC detectors. ToT, as a means to improve the count rate capability at high fluxes, has been demonstrated with an improvement of a factor 3–6, depending on the settings [46]. The count-rate correction equation is expressed as follows:

$$\varphi = \phi \frac{1 - e^{-\phi\tau}}{\phi\tau} \tag{2}$$

with little dependence on the frequency of the clock, as long as it is $\gtrsim 5\tau^{-1}$. It is important to point out that in order to obtain the number of photons, it is necessary to normalize the counter value by the average number of counts per photon of that energy and threshold. The main disadvantage of the ToT approach is the distribution of the 10–100-MHz clock over the whole pixel matrix, which requires power and can generate the digital-to-analog crosstalk, increasing the noise. Optimized clock distribution solutions, such as the digital delay-locked loop (dDLL) [47], can help overcome these bottlenecks.

2.2.2 Retriggering

Retriggering was introduced using DECTRIS in the PILATUS3 detector [17] as a measure to increase the count rate capability and avoid the ambiguities of a paralyzable counter at extremely high photon rates. As the name implies, retriggering works by triggering an additional count after a certain time delay. The delay is started on the crossing of the threshold which gives retriggering a clear advantage over the non-synchronized ToT clock. Retriggering relies on knowing the pulse width for a single photon. The rate correction model is described in [48]:

$$\varphi = \frac{\phi}{e^{-\phi\tau} + \phi\tau_r} \tag{3}$$

where τ_r is the time after which the retrigger is evaluated and an additional signal eventually generated. Ideally $\tau_r = \tau$, but τ_r is usually larger to avoid double counts. The KITE ASIC from DECTRIS has been designed for electron detection, and it can support up to ~70 Mcounts/pixel/s with a 43-keV

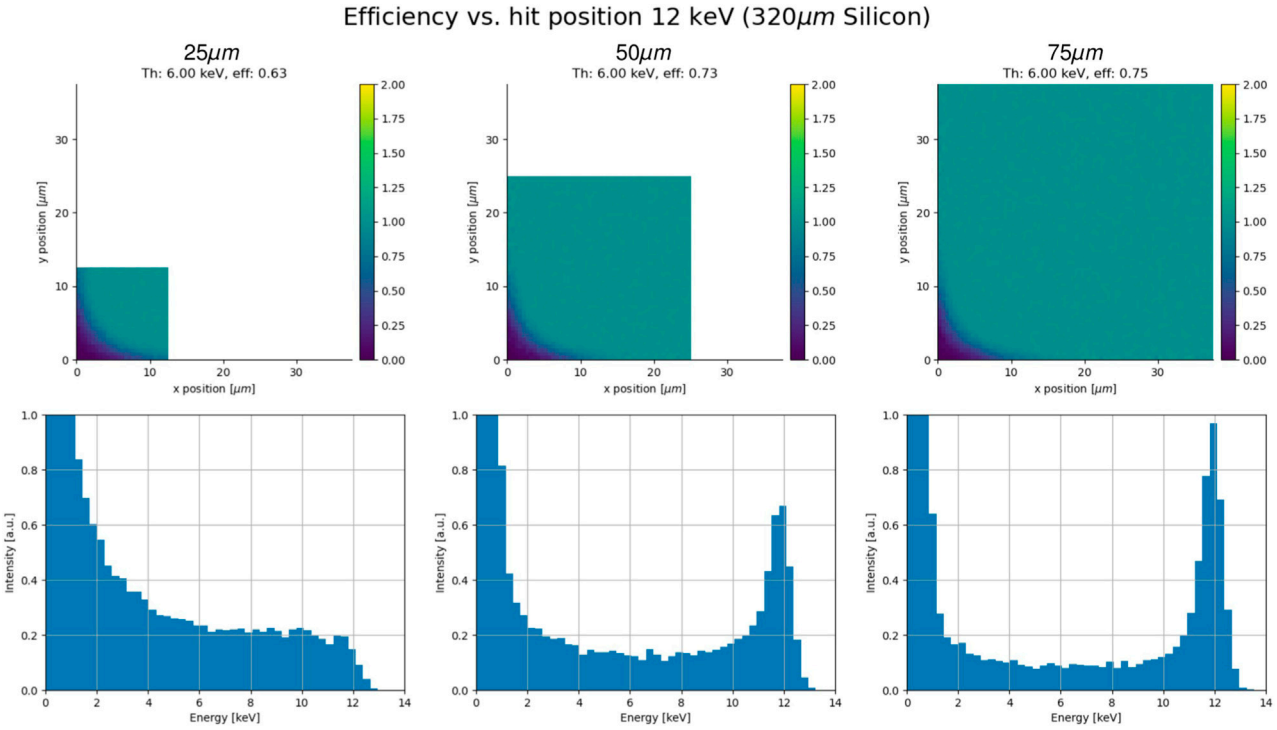

FIGURE 3
Simulation of the detection efficiency and energy response for 25, 50, and 75 μm^2 pixels. As the pixel size shrinks, the corner area gets larger (relative to the rest of the pixel), and both the efficiency and energy response are deteriorated. Photon energy at 12 keV and threshold at 50%. Given the symmetry, only one quarter of the pixel was simulated.

threshold for 200-keV electrons with a 10% loss of counting efficiency compared to approximately 20 Mcounts/pixel/s without retriggering [36].

2.2.3 Pileup tracking

Given a sufficient dynamic range of the front-end, another way to mitigate the loss of efficiency is to use multiple thresholds to count the pileup by placing the additional thresholds above the photon energy (e.g., 1.3 and 1.7 x E_{photon}, as shown in Figure 1F). This method is known as the *pileup trigger method* [49; 50] or *pileup tracking* [51]. Finding the right threshold depends on the analog shape of the signal and sensor geometry (charge sharing). Ideally, also, the higher thresholds are proportional to the energy, similar to the one at half energy. The count rate correction model can be found in [52]:

$$\varphi = \phi \sum_{i=0}^{N} \left(1 - e^{-\phi\tau}\right)^i \tag{4}$$

where N is the number of comparators and counters. The improvement in the count rate capability is very pronounced up to three counters. For additional counters, however, there are diminishing returns, and one also has to consider issues like saturation of the preamplifier and available space in the pixel. The plot shown in Figure 2 refers to three counters. With MYTHEN3 we see an improvement of 4-6x in the count rate at 90% efficiency with three counters. For the new MATTERHORN detector, which is currently at the prototyping stage at PSI, we plan to use this approach with four counters.

2.3 Spatial resolution

Reducing the pixel size is an effective way to limit the incoming photon rate per pixel and improve the spatial resolution but only up to a certain extent. Single-photon counting detectors with relatively large pixels show an ideal MTF [53], when operated with the threshold at half the photon energy. As the pixel size shrinks, the charge cloud, which—in a typical 300-μm-thick silicon sensor—is on the order of 10–20 μm [54], becomes comparable to the pixel size, leading to worse energy response and a loss of detection efficiency in the corners of the pixel. Figure 3 shows a simulation of the energy response and detection efficiency as a function of the interaction position in the pixel for 25, 50, and 75 μm^2 pixels performed using GEANT4 [55] with custom drift-diffusion [56] implementation. As the pixel size becomes smaller, the corner area, where the charge generated by a photon is shared between four pixels, gets larger relative to the rest of the pixel, and both energy response and detection efficiency are degraded. Photons absorbed close to the pixel corner, whose signal does not exceed the 50% energy threshold in any of the four neighboring pixels, will not be detected. For pixels smaller than 30–40 μm, it is not possible to work in the single-photon counting mode without a solution to compensate for charge sharing. Due to the absence of a threshold, charge-integrating detectors do not suffer from the corner effect, giving a flat response throughout the pixel [57].

For high-Z sensor materials (section 2.4.1), reducing the pixel size is even more difficult since the often thicker sensors provide a larger charge cloud, and in addition, X-ray fluorescence in the

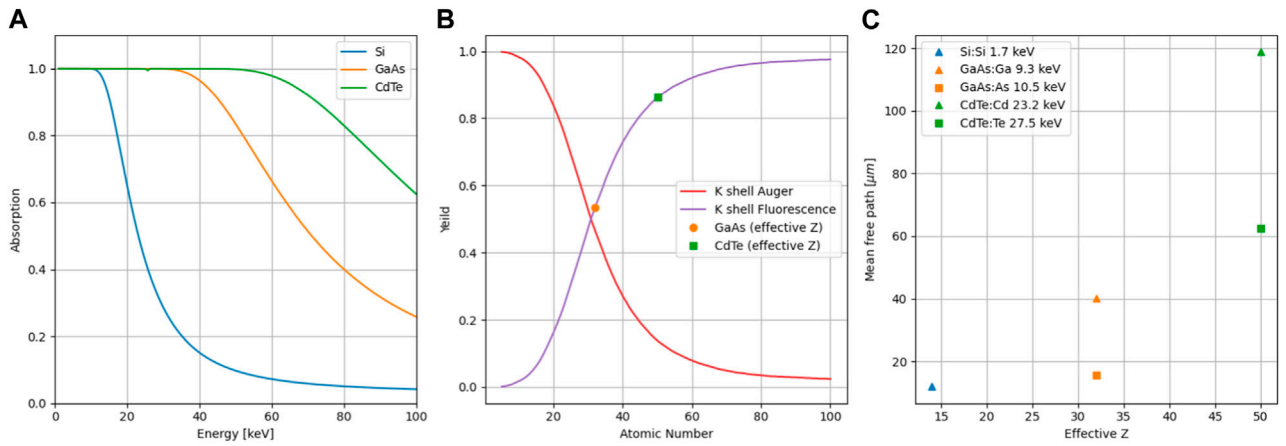

FIGURE 4
(A) X-ray absorption in 1-mm-thick sensors, data obtained from XCOM [100]. **(B)** Auger and K shell fluorescence yield data from [101]. **(C)** Mean free path of K_α fluorescence photons calculated from XCOM data.

material itself further spreads the charge. The fluorescence yield for CdTe is above 80%, and the mean free paths of the characteristic photons are 111 and 58 μm [58]. This leads to distortions in the recorded energy spectrum and additional count rate load since, in many cases, the fluorescence photon is counted separately. Using a charge summing architecture, many of these disadvantages can be overcome [59; 60] but at the cost of the count rate capability [61]. It is possible to handle the corner effect digitally by using multiple comparators and evaluating the coincidence between neighboring pixels. This approach affects the count rate capability similarly to charge summation, but it does not affect the performance of the analog chain.

The best possible spatial resolution of hybrid detectors is reached using a charge-integrating detector under sparse illumination. In this case, charge sharing can be exploited to interpolate between neighboring pixels, reaching a spatial resolution in the micrometer range [62]. For single-photon counting detectors, processing has to happen in the pixel (or strip) since later, no energy information is available. With the MYTHEN3 SPC microstrip detector, it has been demonstrated in 1D that it is possible to use the digital circuitry of a single-photon counting detector with multiple comparators to obtain a spatial resolution better than the physical strip pitch [63]. Similar approaches for pixels are being evaluated, with the additional challenge of a more complex 2D coincidence logic and the need to use a very advanced technology node to shrink the whole circuitry within the necessarily small pixel size [64].

2.4 Advanced sensors

The pulse processing front-end in single-photon counting is more forgiving in terms of leakage current than a charge-integrating front-end and allows the use of sensors with a high and/or variable leakage current since the fluctuations are "filtered" out. This is helpful for detection of both low- and high-energy photons since low-gain avalanche diodes (LGADs) and many high-Z sensors exhibit this behavior. However, to allow full flexibility on the sensor choice, the analog chain of the SPC detector must be designed to work both for hole collection, which is the standard for silicon and inverse LGADs, and electron collection, which is usually required for high-Z sensors and standard LGAD technologies.

2.4.1 High-Z materials

Since silicon becomes almost transparent above 20 keV (see Figure 4A), there is a strong need for sensor materials with higher atomic numbers (i.e., high-Z sensor materials) and thus increased photon cross section. Moving away from silicon, we are faced with intrinsic problems like increased X-ray fluorescence yield and range in the sensor material (Figures 4B,C) but also material defects coming from the fact that it is harder to grow high-quality crystals of compound semiconductors which additionally have not benefited from the massive investment from the electronics industry like silicon.

Over time, GaAs, CdTe, and CZT emerged as the most promising materials, and specifically, CdTe is applicable both for medical imaging [65; 66] and at synchrotrons (among others [67; 68; 69]). Larger-area detectors have also started to appear with, for example, the 16-M CdTe EIGER2X from DECTRIS at the P14 beamline at PETRA III. There was some interest in using germanium for SPC detectors [70], but due to the small band gap, they need to be cooled to $\lesssim$-100°C, complicating the operation. As sensor materials have improved, the focus has shifted from understanding defects like tellurium inclusions [71] to optimizing for high flux and understanding dynamic effects [72; 73]. [74] and [75] offered a good overview of common sensor materials and their use within the Medipix community. At PSI, we have, for example, studied GaAs with JUNGFRAU, probing an effective pixel size and understanding the negative signals observed when used with charge-integrating detectors [76].

In terms of new materials, perovskites [77] have attracted a lot of attention, showing a combination of high atomic number and good mobility-lifetime product. The production cost could be orders of magnitude lower than for CZT/CdTe due to cheap base material and a simpler manufacturing procedure. Although some experiments

have been done with photon counting [78], we are still far from observing large-area perovskite detectors at synchrotrons. One potential issue with the current materials is the relatively low mobility [79], which could cause problems in terms of ballistic deficit at the fast shaping times needed for high count rates.

Looking at high-Z sensor material from the perspective of the readout ASIC, we observe a need for electron collection since most high-Z sensor materials have better transport properties for electrons than holes. Leakage current compensation is also important, given the higher leakage currents in most materials, for example, >200 pA per $75 \times 75\ \mu m^2$ pixel at room temperature using GaAs, as shown in [80]. The pixel size is also limited by the long range of X-ray fluorescence in the sensor layer, for example, 110 μm in CdTe, requiring relatively large pixels even with interpixel communication for an optimal response. If the pixel size goes much below 75 μm, one has to consider events where the fluorescent photon deposits the energy in a pixel that could be several pixels away from the initial interaction.

2.4.2 LGADs

Soft X-ray detection using hybrid detector technology is challenged by the shallow absorption and by the small charge generated by low-energy photons, resulting in low quantum efficiency and low signal-to-noise ratio, respectively. In particular, while charge-integrating detectors can be used for soft X-ray detection even without reaching single-photon resolution, SPC detectors require a SNR $\gtrsim 10$ for single photons, and they are consequently limited to energies above ~2 keV when using standard silicon sensors [28]. The quantum efficiency below 2 keV can be improved by optimizing the entrance window of the silicon sensor, obtaining a performance comparable to state-of-the-art CCDs or CMOS imagers [81].

The signal-to-noise ratio can be improved by exploiting the internal amplification of LGAD sensors recently developed for high-energy physics application. They consist of a silicon sensor with a highly doped p-n junction, where charge carriers are multiplied by impact ionization, thanks to the high electric field. The main goal in particle physics is to use the fast avalanche to improve the timing performance and use the time of arrival of the particle for 4D tracking at high-luminosity colliders [82]. However, the requirements for photon science require additional developments, including small pixels $\lesssim 100\ \mu$m and full sensitivity at the entrance window, in contrast to HEP detectors, with large pads and a thin sensitive layer on a thick substrate. Various LGAD fabrication technologies are described in detail in [83]. A few feasibility studies have been dedicated to X-ray detection [84; 85; 51], aimed at reducing the effective noise, thanks to the multiplication gain, while maximizing the fill factor, which is limited in most LGAD technologies due to the presence of regions without multiplication between the pixels. The performance of LGAD sensors combined with SPC readout electronics does not suffer much from the high leakage current due to the internal amplification, which, however, limits the maximum exposure time acceptable for charge-integrating detectors with LGAD sensors. Recently, the inverse LGAD sensors with optimized entrance window developed by [86] have been combined with the EIGER single-photon counting detector, allowing, for the first time, a SPC pixel detector to reach energies below 1 keV. The low noise and high dynamic range allowed achieving unprecedented data quality in magnetic contrast soft X-ray ptychography, as described by [87].

LGADs can also be exploited for tender and hard X-ray detection to improve the count rate capability using a faster shaping of the analog signal since gain is provided in the sensor, and therefore, the signal can be sacrificed using fast analog settings and accepting a more ballistic deficit.

2.5 Single-photon counting *versus* charge integrating

With the introduction of charge-integrating detectors with dynamic gain switching (like JUNGFRAU Mozzanica et al. [88]), it is possible to measure with an electronic noise below the Poisson limit from a single photon throughout the full dynamic range (10^4 12 keV photons/pixel). The maximum 2 kHz frame rate of JUNGFRAU translates to a count rate capability of approximately 20 Mphotons/pixel/s at 12 keV. Since it is an integrating detector, the maximum supported flux scales inversely with the photon energy, providing even higher numbers at lower energies (e.g., 10^5 photons/pixel/frame and 200 Mphotons/pixel/s at 1.2 keV). Different from SPC detectors, JUNGFRAU is linear throughout the dynamic range independent of the photon rate (e.g., 40 Mphotons/pixel/s at 6 keV). [89] showed that data quality remained high even at full beamline transmission (thaumatin crystal at 6 keV) in contrast to previously published results with an EIGER 1-M detector [14].

For a charge-integrating detector, the highest continuous flux is determined by the dynamic range multiplied by the frame rate. We are currently developing the second-generation JUNGFRAU detector with a target frame rate of 10 kHz, which, given the same dynamic range, could cope with 100 Mphotons/pixel/s at 12 keV. This would provide a solution for the most extreme fluxes at the cost of dealing with 12.5 GB/s per 500 kpixel module. However, since the performance of charge-integrating detectors degrades above a few hundred microseconds integration time (higher noise and lower dynamic range), longer exposure times must be achieved by summing up multiple images, with a consequent increase in the electronic noise, which scales with the square root of the number of frames.

At the other extremes, charge-integrating detectors have their place in photon-starved applications since with a low enough flux, it is possible to measure the charge deposited per pixel per photon, enabling both spectroscopic measurements and interpolation (Bergamaschi et al. [90]). However, in this application, the maximum supported flux is limited by the frame rate of the detector, which is typically of the order of a few kHz with one outstanding exception being the HEXITEC$_{MHz}$ [91]. For the same applications, the implementation of energy binning or a sub-pixel resolution in a single-photon counting chip could increase the maximum supported flux of up to three orders of magnitude since it would be limited by the ~100 ns shaping time rather than by the ~500 μs readout time [63].

An ideal detector should perform like a single-photon counter under low illumination (noiseless, stable, and low frame rate possible) but be capable of supporting high fluxes when

necessary. Charge-integrating detectors with a single-photon resolution converting the analog data to the number of photons on-the-fly and summing up frames to achieve long exposure times promise to achieve this goal, as shown in Leonarski et al. [92], but compared to SPC detectors, they require more developments in terms of chip design, firmware development, and data backend. Moreover, the integration of the leakage current requires the acquisition of frequent dark images to follow possible thermal drifts and the effect of radiation damage, which are usually filtered out in SPC detectors.

2.5.1 Mixed mode

An approach for obtaining ideal behavior from a large detector is to equip the more illuminated area of the detector (e.g., the central region for coherent scattering) with charge-integrating detector modules and a high-performance data back-end system and substitute single-photon counting modules in regions with lower illumination, synchronizing the acquisition of all the modules. Some challenges and artefacts might still arise when combining data from such different detector systems.

Charge removal architectures are a hybrid between single-photon counting and charge-integrating detectors [93; 94]. They have a fully digital readout, and ideally, they can provide a high gain (and low noise) on the whole virtually infinite dynamic range. High-flux detection is possible, only limited by the speed of charge removal (e.g., they are not usable at XFELs), while a slow frame rate readout is still feasible, with the disadvantage of large pedestal corrections due to the integration of the leakage current. Charge removal architectures might suffer from high noise levels at high intensities due to charge injection fluctuations during charge removal.

The possibility to statically configure the detector in the counting or integrating mode depending on the application (or on the illumination level) would add great flexibility, and users could benefit from the advantages of two detector systems, without the need to change the detector. This is possible by adding to the feedback circuit of the preamplifier of a SPC detector a reset switch. When the reset is open and the field-effect transistor (FET) controlling the feedback resistor is active, the detector can be operated in the SPC mode, feeding the preamplifier output to an additional shaper and comparator [95]. When the FET of the feedback resistor is off, the reset can be operated to integrate the charge on the feedback capacitor during the given exposure time and then sample on a storage capacitance. The comparator used in the SPC mode could be used in order to implement dynamic gain switching, while the shaper could be operated similar to the preamplifier for correlated double sampling (CDS). Such an architecture has been implemented and successfully tested in a MYTHEN3 microstrip prototype and will be adapted to pixel detectors. Ideally, the detector should dynamically adapt its behavior depending on the illumination, similar to dynamic gain switching, but this comes with additional challenges in the conversion of the signal into number of photons.

2.6 More photons, more data

Single-photon counting detectors present some advantages from the data handling point of view compared to charge-integrating detectors since the detector readout already consists of the number of detected photons, without the need for additional processing. Moreover, the fully digital readout simplifies the data compression (e.g., zero suppression), making it possible already on the readout board or even on-chip.

Still, the higher frame rates driven by the increased brilliance will be a huge challenge for the beam lines. Already the previous generation detectors kicked off the “data deluge” [96], and with new detectors coming out with unprecedented data rates like MATTERHORN with 100 Gbit/s per 500k pixel module or TIMEPIX4 [97] with 16 × 10 Gbit/s serializers per chip (448 Ã— 512 pixels) saving (or even receiving), all raw data on the computing infrastructure will not be possible. The LEAPS[1] data strategy [98] outlines the importance of involving central IT services to take some of the burden off experimental groups which might not be used for large datasets, but with the explosion of data, we believe that measures also need to be taken to reduce data at the source.

We see two different approaches, of which one is to build a custom receiving system using FPGAs and GPUs to perform local processing like in [92] before streaming out the data, and the other is to move data reduction onto the readout board or even into the ASIC itself. Reducing the data closer to where it is produced has the added benefit that it lowers the demands on subsequent network and computing infrastructure at the cost of flexibility. For now, it remains an open but highly important field, and we need to see what works best in practice.

3 Conclusion

SPC detectors have been the most used position-sensitive detectors at synchrotron facilities for more than a decade, but the higher brilliance of the fourth-generation light sources requires a new generation with improved performance. There are several single-photon counting detectors under development which will be used at diffraction-limited sources including SPHIRD [94], MEDIPIX4 [99], and our own MATTERHORN. All these projects aim to significantly improve their count rate capability compared to existing systems, and in section 2.2, we presented some of the solutions which are being investigated to achieve this goal. Of the compared methods, pileup tracking shows potential to give the highest count rate, but one also has to consider other features of the detector like calibration, correction of mismatches between channels, spectral response, and radiation hardness. Therefore, the best solution will be the one which provides the most accurate data, something that could vary between applications and facilities.

Additional features like the possibility of using multiple comparators and counters and extending the usable energy range from soft X-rays to high-energy photons will open new possibilities for SPC detectors and can eventually pioneer novel experimental

1 League of European Accelerator based Photon Sources https://leaps-initiative.eu/

techniques. Despite not being the optimal solution for targeting high-resolution imaging applications, SPC hybrid detectors with intercommunication between pixels at the analog or at the digital level can further push the spatial resolution or at least improve some of the current flaws of SPC detectors with small pixels, like the corner effect.

Despite the challenge brought by the increased flux, we think that SPC detectors will have a bright future at diffraction-limited light sources and remain the workhorse detector in the near to mid-term future, thanks to their reliability and ease of use. For the highest rate applications, charge-integrating detectors will complement photon counting, until the mixed mode readout combining the advantage of both architecture and other novel readout methods will be available.

Author contributions

EF: conceptualization and writing–original draft. AB: conceptualization and writing–original draft. BS: writing–review and editing.

Funding

The author(s) declare financial support was received for the research, authorship, and/or publication of this article. Open access funding was provided by the PSI—Paul Scherrer Institute.

Conflict of interest

The authors declare that the research was conducted in the absence of any commercial or financial relationships that could be construed as a potential conflict of interest.

Publisher's note

References

1. Heijne E, Jarron P, Olsen A, Redaelli N. The silicon micropattern detector: a dream? *Nucl Instr Methods Phys Res Section A: Acc Spectrometers, Detectors Associated Equipment* (1988) 273:615–9. doi:10.1016/0168-9002(88)90065-4

2. Anghinolfi F, Aspell P, Bass K, Beusch W, Bosisio L, Boutonnet C, et al. A 1006 element hybrid silicon pixel detector with strobed binary output. *IEEE Trans Nucl Sci* (1992) 39:654–61. doi:10.1109/23.159682

3. Alexeev G, Andersen E, Andrighetto A, Antinori F, Armenise N, Ban J, et al. First results from the 1994 lead beam run of wa97. *Nucl Phys A* (1995) 590:139–46. doi:10.1016/0375-9474(95)00232-P

4. Becks K, Borghi P, Brunet J, Caccia M, Clemens J, Cohen-Solal M, et al. The delphi pixels. *Nucl Instr Methods Phys Res Section A: Acc Spectrometers, Detectors Associated Equipment* (1997) 386:11–7. doi:10.1016/S0168-9002(96)01089-3

5. Heijne E, Antinori F, Beker H, Batignani G, Beusch W, Bonvicini V, et al. Development of silicon micropattern pixel detectors. *Nucl Instr Methods Phys Res Section A: Acc Spectrometers, Detectors Associated Equipment* (1994) 348:399–408. doi:10.1016/0168-9002(94)90768-4

6. Da Via C, Bates R, Bertolucci E, Bottigli U, Campbell M, Chesi E, et al. Gallium arsenide pixel detectors for medical imaging. *Nucl Instr Methods Phys Res Section A: Acc Spectrometers, Detectors Associated Equipment* (1997) 395:148–51. doi:10.1016/S0168-9002(97)00631-1

7. Campbell M, Heijne E, Meddeler G, Pernigotti E, Snoeys W. A readout chip for a 64/spl times/64 pixel matrix with 15-bit single photon counting. *IEEE Trans Nucl Sci* (1998) 45:751–3. doi:10.1109/23.682629

8. Delpierre P, Berar J, Blanquart L, Caillot B, Clemens J, Mouget C. X-ray pixel detector for crystallography. *IEEE Trans Nucl Sci* (2001) 48:987–91. doi:10.1109/23.958710

9. Brönnimann C, Baur R, Eikenberry E, Kohout S, Lindner M, Schmitt B, et al. A pixel read-out chip for the pilatus project. *Nucl Instr Methods Phys Res Section A: Acc Spectrometers, Detectors Associated Equipment* (2001) 465:235–9. doi:10.1016/s0168-9002(01)00396-5

10. Kästli H, Barbero M, Erdmann W, Hörmann C, Horisberger R, Kotlinski D, et al. Design and performance of the cms pixel detector readout chip. *Nucl Instr Methods Phys Res Section A: Acc Spectrometers, Detectors Associated Equipment* (2006) 565:188–94. doi:10.1016/j.nima.2006.05.038

11. Broennimann C, Eikenberry EF, Henrich B, Horisberger R, Huelsen G, Pohl E, et al. The PILATUS 1M detector. *J Synchrotron Radiat* (2006) 13:120–30. doi:10.1107/S0909049505038665

12. Pflugrath JW. The finer things in x-ray diffraction data collection. *Acta Crystallogr Section D* (1999) 55:1718–25. doi:10.1107/s090744499900935x

13. Förster A, Brandstetter S, Schulze-Briese C. Transforming x-ray detection with hybrid photon counting detectors. *Philos Trans R Soc A* (2019) 377:20180241. doi:10.1098/rsta.2018.0241

14. Casanas A, Warshamanage R, Finke AD, Panepucci E, Olieric V, Nöll A, et al. Eiger detector: application in macromolecular crystallography. *Acta Crystallogr* (2016) D72:1036–48. doi:10.1107/s2059798316012304

15. Pfeiffer F. X-ray ptychography. *Nat Photon* (2018) 12:9–17. doi:10.1038/s41566-017-0072-5

16. Kraft P, Bergamaschi A, Broennimann C, Dinapoli R, Eikenberry EF, Henrich B, et al. Performance of single-photon-counting PILATUS detector modules. *J Synchrotron Radiat* (2009) 16:368–75. doi:10.1107/S0909049509009911

17. Loeliger T, Brönnimann C, Donath T, Schneebeli M, Schnyder R, Trüb P. The new pilatus3 asic with instant retrigger capability. In: Proceedings of the 2012 IEEE Nuclear Science Symposium and Medical Imaging Conference Record (NSS/MIC); November 2012; Anaheim, CA, USA (2012). p. 610–5. doi:10.1109/NSSMIC.2012.6551180

18. Johnson I, Bergamaschi A, Buitenhuis J, Dinapoli R, Greiffenberg D, Henrich B, et al. Capturing dynamics with Eiger, a fast-framing X-ray detector. *J Synchrotron Radiat* (2012) 19:1001–5. doi:10.1107/S0909049512035972

19. Donath T, Šišak Jung D, Burian M, Radicci V, Zambon P, Fitch AN, et al. EIGER2 hybrid-photon-counting X-ray detectors for advanced synchrotron diffraction experiments. *J Synchrotron Radiat* (2023) 30:723–38. doi:10.1107/S160057752300454X

20. Medjoubi K, Bucaille T, Hustache S, Bérar J-F, Boudet N, Clemens J-C, et al. Detective quantum efficiency, modulation transfer function and energy resolution comparison between CdTe and silicon sensors bump-bonded to XPAD3S. *J Synchrotron Radiat* (2010) 17:486–95. doi:10.1107/S0909049510013257

21. Bachiller-Perea D, Abiven Y-M, Bisou J, Fertey P, Grybos P, Jarnac A, et al. First pump–probe–probe hard X-ray diffraction experiments with a 2D hybrid pixel detector developed at the SOLEIL synchrotron. *J Synchrotron Radiat* (2020) 27:340–50. doi:10.1107/S1600577520000612

22. Nakaye Y, Sakumura T, Sakuma Y, Mikusu S, Dawiec A, Orsini F, et al. Characterization and performance evaluation of the XSPA-500k detector using synchrotron radiation. *J Synchrotron Radiat* (2021) 28:439–47. doi:10.1107/S1600577520016665

23. Ponchut C, Rigal JM, Clément J, Papillon E, Homs A, Petitdemange S. Maxipix, a fast readout photon-counting x-ray area detector for synchrotron applications. *J Instrumentation* (2011) 6:C01069. doi:10.1088/1748-0221/6/01/C01069

24. Pennicard D, Lange S, Smoljanin S, Becker J, Hirsemann H, Epple M, et al. Development of lambda: large area medipix-based detector array. *J Instrumentation* (2011) 6:C11009. doi:10.1088/1748-0221/6/11/C11009

25. Tartoni N, Dennis G, Gibbons P, Gimenez E, Horswell I, Marchal J, et al. Excalibur: a three million pixels photon counting area detector for coherent diffraction imaging based on the medipix3 asic. In: Proceedings of the 2012 IEEE Nuclear Science Symposium and Medical Imaging Conference Record (NSS/MIC); November 2012; Anaheim, CA, USA (2012). p. 530–3. doi:10.1109/NSSMIC.2012.6551164

26. Bergamaschi A, Cervellino A, Dinapoli R, Gozzo F, Henrich B, Johnson I, et al. The MYTHEN detector for X-ray powder diffraction experiments at the Swiss Light Source. *J Synchrotron Radiat* (2010) 17:653–68. doi:10.1107/S0909049510026051

27. Tinti G, Marchetto H, Vaz CAF, Kleibert A, Andrä M, Barten R, et al. The EIGER detector for low-energy electron microscopy and photoemission electron microscopy. *J Synchrotron Radiat* (2017) 24:963–74. doi:10.1107/S1600577517009109

28. Andrä M, Barten R, Bergamaschi A, Brückner M, Casati N, Cervellino A, et al. Towards mythen iii - prototype characterisation of mythen iii.0.2. *J Instrumentation* (2019) 14:C11028. doi:10.1088/1748-0221/14/11/C11028

29. Kraft P, Bergamaschi A, Bronnimann C, Dinapoli R, Eikenberry EF, Graafsma H, et al. Characterization and calibration of pilatus detectors. *IEEE Trans Nucl Sci* (2009) 56:758–64. doi:10.1109/TNS.2008.2009448

30. Maj P, Grybos P, Kmon P, Szczygiel R. 23552-channel ic for single photon counting pixel detectors with 75 μ m pitch, enc of 89 e rms, 19 e rms offset spread and 3 spread. In: Proceedings of the ESSCIRC 2014 - 40th European Solid State Circuits Conference (ESSCIRC); September 2014; Venice Lido, Italy (2014). p. 147–50. doi:10.1109/ESSCIRC.2014.6942043

31. Ponchut C, Visschers J, Fornaini A, Graafsma H, Maiorino M, Mettivier G, et al. Evaluation of a photon-counting hybrid pixel detector array with a synchrotron x-ray source. *Nucl Instr Methods Phys Res Section A: Acc Spectrometers, Detectors Associated Equipment* (2002) 484:396–406. doi:10.1016/S0168-9002(01)02029-0

32. Niederlöhner D, Bert C, Giersch J, Pfeiffer K-F, Anton G. Threshold characterisation of the medipix1 chip. *Nucl Instr Methods Phys Res Section A: Acc Spectrometers, Detectors Associated Equipment* (2003) 509:138–45. doi:10.1016/S0168-9002(03)01562-6

33. Bergamaschi A, Cervellino A, Dinapoli R, Gozzo F, Henrich B, Johnson I, et al. Photon counting microstrip detector for time resolved powder diffraction experiments. *Nucl Instr Methods Phys Res Section A: Acc Spectrometers, Detectors Associated Equipment* (2009) 604:136–9. doi:10.1016/j.nima.2009.01.092

34. Swank RK. Absorption and noise in x-ray phosphors. *J Appl Phys* (1973) 44:4199–203. doi:10.1063/1.1662918

35. Hocine S, Van Swygenhoven H, Van Petegem S, Chang CST, Maimaitiyili T, Tinti G, et al. Operando x-ray diffraction during laser 3d printing. *Mater Today* (2020) 34:30–40. doi:10.1016/j.mattod.2019.10.001

36. Zambon P, Bottinelli S, Schnyder R, Musarra D, Boye D, Dudina A, et al. Kite: high frame rate, high count rate pixelated electron counting asic for 4d stem applications featuring high-z sensor. *Nucl Instr Methods Phys Res Section A: Acc Spectrometers, Detectors Associated Equipment* (2023) 1048:167888. doi:10.1016/j.nima.2022.167888

37. König H-H, Pettersson NH, Durga A, Van Petegem S, Grolimund D, Chuang AC, et al. Solidification modes during additive manufacturing of steel revealed by high-speed x-ray diffraction. *Acta Materialia* (2023) 246:118713. doi:10.1016/j.actamat.2023.118713

38. Burian M, Marmiroli B, Radeticchio A, Morello C, Naumenko D, Biasiol G, et al. Picosecond pump–probe X-ray scattering at the Elettra SAXS beamline. *J Synchrotron Radiat* (2020) 27:51–9. doi:10.1107/S1600577519015728

39. Ballabriga R, Alozy J, Campbell M, Frojdh E, Heijne E, Koenig T, et al. Review of hybrid pixel detector readout asics for spectroscopic x-ray imaging. *J Instrumentation* (2016) 11:P01007. doi:10.1088/1748-0221/11/01/P01007

40. Lowe C. *WhitePaper_Draft10.pdf* (2021). doi:10.6084/m9.figshare.13541051.v1

41. Naumenko D, Burian M, Marmiroli B, Haider R, Radeticchio A, Wagner L, et al. Implication of the double-gating mode in a hybrid photon counting detector for measurements of transient heat conduction in GaAs/AlAs superlattice structures. *J Appl Crystallogr* (2023) 56:961–6. doi:10.1107/S1600576723004302

42. Grybos P, Kleczek R, Kmon P, Otfinowski P, Fajardo P, Magalhães D, et al. Sphird–single photon counting pixel readout asic with pulse pile-up compensation methods. *IEEE Trans Circuits Syst Express Briefs* (2023) 70:3248–52. doi:10.1109/TCSII.2023.3267859

43. Trueb P, Dejoie C, Kobas M, Pattison P, Peake DJ, Radicci V, et al. Bunch mode specific rate corrections for PILATUS3 detectors. *J Synchrotron Radiat* (2015) 22:701–7. doi:10.1107/S1600577515003288

44. Leo WR. *Techniques for nuclear and particle physics experiments: a how-to approach*. 2nd ed. Berlin: Springer (1994). doi:10.1007/978-3-642-57920-2

45. Llopart X, Ballabriga R, Campbell M, Tlustos L, Wong W. Timepix, a 65k programmable pixel readout chip for arrival time, energy and/or photon counting measurements. *Nucl Instr Methods Phys Res Section A: Acc Spectrometers, Detectors Associated Equipment* (2007) 581:485–94. doi:10.1016/j.nima.2007.08.079

46. Bergamaschi A, Dinapoli R, Greiffenberg D, Henrich B, Johnson I, Mozzanica A, et al. Time-over-threshold readout to enhance the high flux capabilities of single-photon-counting detectors. *J Synchrotron Radiat* (2011) 18:923–9. doi:10.1107/S0909049511034480

47. Llopart X, Alozy J, Ballabriga R, Campbell M, Egidos N, Fernandez J, et al. Study of low power front-ends for hybrid pixel detectors with sub-ns time tagging. *J Instrumentation* (2019) 14:C01024. doi:10.1088/1748-0221/14/01/C01024

48. Zambon P. Dead time model for x-ray photon counting detectors with retrigger capability. *Nucl Instr Methods Phys Res Section A: Acc Spectrometers, Detectors Associated Equipment* (2021) 994:165087. doi:10.1016/j.nima.2021.165087

49. Kappler S, Hölzer S, Kraft E, Stierstorfer K, Flohr T. Quantum-counting CT in the regime of count-rate paralysis: introduction of the pile-up trigger method. *Proc SPIE - Int Soc Opt Eng* (2011) 7961:79610T. doi:10.1117/12.877939

50. Kraft E, Glasser F, Kappler S, Niederloehner D, Villard P. Experimental evaluation of the pile-up trigger method in a revised quantum-counting CT detector. In: Proceedings of the Medical Imaging 2012: Physics of Medical Imaging; San Diego, California (2012). p. 83134A. doi:10.1117/12.911231

51. Andrä M, Zhang J, Bergamaschi A, Barten R, Borca C, Borghi G, et al. Development of low-energy X-ray detectors using LGAD sensors. *J Synchrotron Radiat* (2019) 26:1226–37. doi:10.1107/S1600577519005393

52. Andrä M. *The MYTHEN III Detector System - a single photon-counting microstrip detector for powder diffraction experiments*. Phd thesis. Zürich, Switzerland: ETH Zürich (2021). Available at: http://hdl.handle.net/20.500.11850/462676.

53. Donath T, Brandstetter S, Cibik L, Commichau S, Hofer P, Krumrey M, et al. Characterization of the pilatus photon-counting pixel detector for x-ray energies from 1.75 kev to 60 kev. *J Phys Conf Ser* (2013) 425:062001. doi:10.1088/1742-6596/425/6/062001

54. Bergamaschi A, Cartier S, Dinapoli R, Greiffenberg D, Jungmann-Smith J, Mezza D, et al. Looking at single photons using hybrid detectors. *J Instrumentation* (2015) 10:C01033. doi:10.1088/1748-0221/10/01/C01033

55. Agostinelli S, Allison J, Amako K, Apostolakis J, Araujo H, Arce P, et al. Geant4—a simulation toolkit. *Nucl Instr Methods Phys Res Section A: Acc Spectrometers, Detectors Associated Equipment* (2003) 506:250–303. doi:10.1016/S0168-9002(03)01368-8

56. Schübel A, Krapohl D, Fröjdh E, Fröjdh C, Thungström G. A geant4 based framework for pixel detector simulation. *J Instrumentation* (2014) 9:C12018. doi:10.1088/1748-0221/9/12/C12018

57. Leonarski F, Redford S, Mozzanica A, Lopez-Cuenca C, Panepucci E, Nass K, et al. Fast and accurate data collection for macromolecular crystallography using the jungfrau detector. *Nat Methods* (2018) 15:799–804. doi:10.1038/s41592-018-0143-7

58. Tlustos L. *Performance and limitations of high granularity single photon processing X-ray imaging detectors* (2005).

59. Gimenez EN, Ballabriga R, Campbell M, Horswell I, Llopart X, Marchal J, et al. Study of charge-sharing in medipix3 using a micro-focused synchrotron beam. *J Instrumentation* (2011) 6:C01031. doi:10.1088/1748-0221/6/01/C01031

60. Koenig T, Zuber M, Hamann E, Cecilia A, Ballabriga R, Campbell M, et al. How spectroscopic x-ray imaging benefits from inter-pixel communication. *Phys Med Biol* (2014) 59:6195–213. doi:10.1088/0031-9155/59/20/6195

61. Frojdh E, Ballabriga R, Campbell M, Fiederle M, Hamann E, Koenig T, et al. Count rate linearity and spectral response of the medipix3rx chip coupled to a 300 μm silicon sensor under high flux conditions. *J Instrumentation* (2014) 9:C04028. doi:10.1088/1748-0221/9/04/C04028

62. Cartier S, Kagias M, Bergamaschi A, Wang Z, Dinapoli R, Mozzanica A, et al. Micrometer-resolution imaging using MÖNCH: towards G_2-less grating interferometry. *J Synchrotron Radiat* (2016) 23:1462–73. doi:10.1107/S1600577516014788

63. Bergamaschi A, Andrä M, Barten R, Baruffaldi F, Brückner M, Carulla M, et al. First demonstration of on-chip interpolation using a single photon counting microstrip detector. *J Instrumentation* (2022) 17:C11012. doi:10.1088/1748-0221/17/11/C11012

64. Krzyzanowska A, Szczygiel R, Grybos P, Koczwara J, Cislo K, Stasiak A Charge sharing simulations and measurements for digital algorithms aiming at subpixel resolution in photon counting pixel detectors. *J Instrumentation* (2023) 18:C02024. doi:10.1088/1748-0221/18/02/C02024

65. Flohr T, Petersilka M, Henning A, Ulzheimer S, Ferda J, Schmidt B. Photon-counting ct review. *Physica Med* (2020) 79:126–36. doi:10.1016/j.ejmp.2020.10.030

66. Holmes TW, Liu LP, Shapira N, McVeigh E, Litt HI, Pourmorteza A, et al. Mixed coronary plaque characterization with the first clinical dual-source photon-counting CT scanner: a phantom study. In: Stayman JW, editor. Proceedings of the 7th International Conference on Image Formation in X-Ray Computed Tomography. International Society for Optics and Photonics SPIE (2022). p. 123041U. doi:10.1117/12.2647009

67. Brombal L, Donato S, Brun F, Delogu P, Fanti V, Oliva P, et al. Large-area single-photon-counting CdTe detector for synchrotron radiation computed tomography: a dedicated pre-processing procedure. *J Synchrotron Radiat* (2018) 25:1068–77. doi:10.1107/S1600577518006197

68. Krause L, Tolborg K, Grønbech TBE, Sugimoto K, Iversen BB, Overgaard J. Accurate high-resolution single-crystal diffraction data from a Pilatus3X CdTe detector. *J Appl Crystallogr* (2020) 53:635–49. doi:10.1107/S1600576720003775

69. Aslandukov A, Aslandukova A, Laniel D, Koemets I, Fedotenko T, Yuan L, et al. High-pressure yttrium nitride, y5n14, featuring three distinct types of nitrogen dimers. *The J Phys Chem C* (2021) 125:18077–84. doi:10.1021/acs.jpcc.1c06210

70. Pennicard D, Struth B, Hirsemann H, Sarajlic M, Smoljanin S, Zuvic M, et al. A germanium hybrid pixel detector with 55m pixel size and 65,000 channels. *J Instrumentation* (2014) 9:P12003. doi:10.1088/1748-0221/9/12/P12003

71. Bolotnikov AE, Abdul-Jabbar NM, Babalola OS, Camarda GS, Cui Y, Hossain AM, et al. Effects of te inclusions on the performance of cdznte radiation detectors. *IEEE Trans Nucl Sci* (2008) 55:2757–64. doi:10.1109/TNS.2008.2003355

72. Baussens O, Ponchut C, Ruat M, Bettelli M, Zanettini S, Zappettini A. Characterization of high-flux cdznte with optimized electrodes for 4th generation

synchrotrons. *J Instrumentation* (2022) 17:C11008. doi:10.1088/1748-0221/17/11/C11008

73. Iniewski K. Czt detector technology for medical imaging. *J Instrumentation* (2014) 9:C11001. doi:10.1088/1748-0221/9/11/C11001

74. Pennicard D, Pirard B, Tolbanov O, Iniewski K. Semiconductor materials for x-ray detectors. *MRS Bull* (2017) 42:445–50. doi:10.1557/mrs.2017.95

75. Fiederle M, Procz S, Hamann E, Fauler A, Fröjdh C. Overview of gaas und cdte pixel detectors using medipix electronics. *Cryst Res Tech* (2020) 55:2000021. doi:10.1002/crat.202000021

76. Greiffenberg D, Andrä M, Barten R, Bergamaschi A, Busca P, Brückner M, et al. Characterization of gaas:cr sensors using the charge-integrating jungfrau readout chip. *J Instrumentation* (2019) 14:P05020. doi:10.1088/1748-0221/14/05/P05020

77. Wei H, Huang J. Halide lead perovskites for ionizing radiation detection. *Nat Commun* (2019) 10:1066. doi:10.1038/s41467-019-08981-w

78. Pan L, He Y, Klepov VV, De Siena MC, Kanatzidis MG. Perovskite cspbbr3 single crystal detector for high flux x-ray photon counting. *IEEE Trans Med Imaging* (2022) 41:3053–61. doi:10.1109/TMI.2022.3176801

79. Wei H, DeSantis D, Wei W, Deng Y, Guo D, Savenije TJ, et al. Dopant compensation in alloyed ch3nh3pbbr3-x cl x perovskite single crystals for gamma-ray spectroscopy. *Nat Mater* (2017) 16:826–33. doi:10.1038/nmat4927

80. Greiffenberg D, Andrä M, Barten R, Bergamaschi A, Brückner M, Busca P, et al. Characterization of chromium compensated gaas sensors with the charge-integrating jungfrau readout chip by means of a highly collimated pencil beam. *Sensors* (2021) 21:1550. doi:10.3390/s21041550

81. Carulla M, Vignali MC, Barten R, Baruffaldi F, Bergamaschi A, Borghi G, et al. Study of the internal quantum efficiency of fbk sensors with optimized entrance windows. *J Instrumentation* (2023) 18:C01073. doi:10.1088/1748-0221/18/01/C01073

82. Cartiglia N, Arcidiacono R, Borghi G, Boscardin M, Costa M, Galloway Z, et al. Lgad designs for future particle trackers. *Nucl Instr Methods Phys Res Section A: Acc Spectrometers, Detectors Associated Equipment* (2020) 979:164383. doi:10.1016/j.nima.2020.164383

83. Giacomini G. Lgad-based silicon sensors for 4d detectors. *Sensors* (2023) 23:2132. doi:10.3390/s23042132

84. Moffat N, Bates R, Bullough M, Flores L, Maneuski D, Simon L, et al. Low gain avalanche detectors (lgad) for particle physics and synchrotron applications. *J Instrumentation* (2018) 13:C03014. doi:10.1088/1748-0221/13/03/c03014

85. Galloway Z, Gee C, Mazza S, Ohldag H, Rodriguez R, Sadrozinski H-W, et al. Use of "lgad" ultra-fast silicon detectors for time-resolved low-kev x-ray science. *Nucl Instr Methods Phys Res Section A: Acc Spectrometers, Detectors Associated Equipment* (2019) 923:5–7. doi:10.1016/j.nima.2019.01.050

86. Zhang J, Barten R, Baruffaldi F, Bergamaschi A, Borghi G, Boscardin M, et al. Development of lgad sensors with a thin entrance window for soft x-ray detection. *J Instrumentation* (2022) 17:C11011. doi:10.1088/1748-0221/17/11/C11011

87. Butcher TA, Phillips NW, Chiu C-C, Wei C-C, Ho S-Z, Chen Y-C, et al. *Ptychographic nanoscale imaging of the magnetoelectric coupling in freestanding bifeo3* (2023).

88. Mozzanica A, Bergamaschi A, Brueckner M, Cartier S, Dinapoli R, Greiffenberg D, et al. Characterization results of the jungfrau full scale readout asic. *J Instrum* (2016) 11:C02047. doi:10.1088/1748-0221/11/02/c02047

89. Leonarski F, Redford S, Mozzanica A, Lopez-Cuenca C, Panepucci E, Nass K, et al. Fast and accurate data collection for macromolecular crystallography using the jungfrau detector. *Nat Commun* (2018) 15:799–804. doi:10.1038/s41592-018-0143-7

90. Bergamaschi A, Andrä M, Barten R, Borca C, Brückner M, Chiriotti S, et al. The mÖnch detector for soft x-ray, high-resolution, and energy resolved applications. *Synchrotron Radiat News* (2018) 31:11–5. doi:10.1080/08940886.2018.1528428

91. Cline B, Banks D, Bell S, Church I, Cross S, Davis A, et al. Characterisation of hexitecmhz - a 1 mhz continuous frame rate spectroscopic x-ray imaging detector system. *Nucl Instr Methods Phys Res Section A: Acc Spectrometers, Detectors Associated Equipment* (2023) 1057:168718. doi:10.1016/j.nima.2023.168718

92. Leonarski F, Brückner M, Lopez-Cuenca C, Mozzanica A, Stadler H-C, Matěj Z, et al. Jungfraujoch: hardware-accelerated data-acquisition system for kilohertz pixel-array X-ray detectors. *J Synchrotron Radiat* (2023) 30:227–34. doi:10.1107/S1600577522010268

93. Weiss JT, Shanks KS, Philipp HT, Becker J, Chamberlain D, Purohit P, et al. High dynamic range x-ray detector pixel architectures utilizing charge removal. *IEEE Trans Nucl Sci* (2017) 64:1101–7. doi:10.1109/TNS.2017.2679540

94. Fajardo P, Busca P, Erdinger F, Fischer P, Ruat M, Schimansky D. Digital integration: a novel readout concept for xider, an x-ray detector for the next generation of synchrotron radiation sources. *J Instrumentation* (2020) 15:C01040. doi:10.1088/1748-0221/15/01/C01040

95. Shi X, Tinti G, Dinapoli R, Mozzanica A, Schmitt B. *Dual mode detector, european patent application ep4042204a1* (2020).

96. Wang C, Steiner U, Sepe A. Synchrotron big data science. *Small* (2018) 14:1802291. doi:10.1002/smll.201802291

97. Llopart X, Alozy J, Ballabriga R, Campbell M, Casanova R, Gromov V, et al. Timepix4, a large area pixel detector readout chip which can be tiled on 4 sides providing sub-200 ps timestamp binning. *J Instrumentation* (2022) 17:C01044. doi:10.1088/1748-0221/17/01/C01044

98. Götz A, le Gall E, Konrad U, Kourousias G, Knodel O, Matalgah S, et al. Leaps data strategy. *The Eur Phys J Plus* (2023) 138:617. doi:10.1140/epjp/s13360-023-04189-6

99. Sriskaran V (2022). *Medipix4, a high granularity four sides buttable pixel readout chip for high resolution spectroscopic x-ray imaging at rates compatible with medical ct scans*. doi:10.5075/epfl-thesis-8617

100. Berger MJ, H Hubbell J, Olsen K. *Xcom: photon cross section database (version 1.5)* (2010).

101. Krause MO. Atomic radiative and radiationless yields for K and L shells. *J Phys Chem Reference Data* (1979) 8:307–27. doi:10.1063/1.555594